
This is the **accepted version** of the journal article:

Gao, Shan. «An earlier start of the thermal growing season enhances tree growth in cold humid areas but not in dry areas». *Nature Ecology & Evolution*, Published online February 2022. DOI 10.1038/s41559-022-01668-4

This version is available at <https://ddd.uab.cat/record/257156>

under the terms of the  **CC BY** COPYRIGHT license

1 **An earlier start of the thermal growing season enhances tree growth in**
2 **cold humid areas but not in dry areas**

3 Shan Gao¹, Eryuan Liang^{1*}, Ruishun Liu¹, Flurin Babst^{2,3}, J. Julio Camarero⁴, Yongshuo H. Fu⁵, Shilong
4 Piao^{1,6}, Sergio Rossi^{7,8}, Miaogen Shen⁹, Tao Wang¹, Josep Peñuelas^{10,11}

5 **Affiliations:**

6 ¹State Key Laboratory of Tibetan Plateau Earth System, Resources and Environment (TPESRE), Institute
7 of Tibetan Plateau Research, Chinese Academy of Sciences, Beijing 100101, China

8 ²School of Natural Resources and the Environment, University of Arizona, Tucson, USA

9 ³Laboratory of Tree-Ring Research, University of Arizona, 1215 E. Lowell St., Tucson, AZ 85721, USA

10 ⁴Instituto Pirenaico de Ecología (IPE-CSIC), 50059 Zaragoza, Spain

11 ⁵College of Water Sciences, Beijing Normal University, Beijing 100875, China

12 ⁶Sino-French Institute for Earth System Science, College of Urban and Environmental Sciences, Peking
13 University, Beijing 100871, China

14 ⁷Département des Sciences Fondamentales, Université du Québec à Chicoutimi, Chicoutimi, Quebec,
15 Canada

16 ⁸Key Laboratory of Vegetation Restoration and Management of Degraded Ecosystems, Guangdong
17 Provincial Key Laboratory of Applied Botany, South China Botanical Garden, Chinese Academy of
18 Sciences, Guangzhou 510650, China

19 ⁹State Key Laboratory of Earth Surface Processes and Resource Ecology, Faculty of Geographical Science,
20 Beijing Normal University, Beijing 100875, China

21 ¹⁰CREAF, Cerdanyola del Valles, Barcelona 08193, Catalonia, Spain

22 ¹¹CSIC, Global Ecology Unit CREAM-CSIC-UAB, Barcelona 08193, Catalonia, Spain

23 * **Correspondence:** Eryuan Liang. Email: liangey@itpcas.ac.cn

24

25 **Abstract**

26 Climatic warming alters the onset, duration and cessation of the vegetative season. While prior studies have
27 shown a tight link between thermal conditions and leaf phenology, less is known about the impacts of
28 phenological changes on tree growth. Here, we assessed the relationships between the start of the thermal
29 growing season (TSOS) and tree growth across the extratropical Northern Hemisphere using 3451 tree-ring
30 chronologies and daily climatic data for 1948-2014. An earlier TSOS promoted growth in regions with high
31 ratios of precipitation to temperature but limited growth in cold dry regions. Path analyses indicated that an
32 earlier TSOS enhanced growth primarily by alleviating thermal limitations on wood formation in boreal
33 forests and by lengthening the period of growth in temperate and Mediterranean forests. Semi-arid and dry
34 subalpine forests, however, did not benefit from an earlier onset of growth and a longer growing season,
35 presumably due to associated water loss and/or more frequent early spring frosts. These emergent patterns
36 of how climatic impacts on wood phenology affect tree growth at regional to hemispheric scales hint at
37 how future phenological changes may affect the carbon sequestration capacity of extratropical forest
38 ecosystems.

39

40 **Main text**

41 **Introduction**

42 An unprecedented increase in temperature has been recorded in recent decades, with higher rates of
43 warming outside than during the main growing season¹. Such warming causes large changes in the timing,
44 duration and thermal conditions of the vegetative season in extratropical terrestrial biomes²⁻⁵. The start of
45 the thermal growing season (TSOS) directly influences vegetation phenology and its advance closely
46 matches the interannual variability of spring green-up⁶⁻¹². These phenological shifts influence the capacity
47 of the biosphere to take up carbon¹³⁻¹⁵ and affect the exchange of energy between the atmosphere and the
48 biosphere^{13, 16}. It remains to be answered, whether the shifts in plant phenology would result in a negative
49 feedback to warming and an increase carbon uptake or alternatively exhibit additional ecological stress¹³.
50 Solving this issue may help reduce uncertainties associated with the forecasting and modeling of forest
51 productivity and global carbon cycling.

52 Satellite observations of forested areas provide evidence that recent climate change has shifted foliar
53 phenology and photosynthetic seasonality¹⁷. Ninety-five percent of the global land surface underwent
54 substantial changes in foliar phenology between 1980 and 2012, including changes in the timing of
55 phenological cycles and the vigor of vegetative activity⁷. In addition to the direct response of an advanced
56 foliar flush to an earlier TSOS¹⁸, peak photosynthesis occurs earlier and culminates higher in forests of the
57 extratropical Northern Hemisphere^{8, 19, 20}. These phenological shifts may be strongly correlated with the
58 thermal conditions in spring, because satellite data indicate that the rate of phenological change slowed
59 under the warming hiatus of 1998-2012²¹.

60 Changes in the timing and vigor of vegetation activity further affect when and how carbon is
61 assimilated by terrestrial ecosystems. The spring shifts of vegetation activity may increase ecosystem
62 productivity due to an earlier start of carbon uptake¹⁹ and longer vegetative seasons with more vigorous
63 photosynthetic activity^{15, 22}. Widespread and contrasting responses of productivity to shifts in foliar
64 phenology, however, have been detected across northern terrestrial ecosystems. The beneficial effects of
65 spring warmth on growing-season productivity can be offset by water stress due to higher
66 evapotranspiration in the summer²³⁻²⁵ and by increasing carbon losses due to higher respiration in the

67 autumn²⁶. A long-term study of biomass also found that alpine plants grew earlier and faster, but the
68 increase in spring productivity was offset by a reduction in autumnal productivity due to increased water
69 stress²⁷. Thus, any attempt to explain climatic influences on terrestrial carbon uptake solely based on
70 studies of shifting foliar phenology and photosynthetic seasonality remains challenging.

71 The carbon residence time in tree stems is much longer than in foliage, making the former a major
72 contributor to the long-term carbon sink in forests²⁸. Tree radial growth represents the annual accumulation
73 and fixation of carbohydrates in the stem. Importantly, wood phenology, mainly in cold areas, is closely
74 related to temperature²⁹. Wood formation in conifers begins when specific critical temperatures and
75 photoperiods are reached³⁰⁻³². In addition to temperature, the length of the growing season determines the
76 available period for developing functional xylem through cell maturation and lignification, especially in
77 cold areas^{31, 33}. In drier ecosystems, water availability for roots, rather than rainfall per se, is another
78 important driver of cambial reactivation³⁴. Temperature and the availability and demand of water also co-
79 determine the rate of growth³⁵⁻³⁷. In addition to climate, the phenology of wood formation is also
80 associated with physiological trade-offs with bud and foliar phenology, because phytohormones produced
81 in developing buds and foliage regulate the rate of cambial division^{29, 38} and can lead to changes in
82 priorities for allocating carbon within a tree.

83 Fundamental but still unresolved questions are thus whether and how the advance of the thermal
84 growing season in spring influences annual tree growth (and biomass accumulation) across environmental
85 gradients. We addressed these questions by investigating the influence of TSOS on tree radial growth
86 (represented by a ring-width index, RWI) in the extratropical Northern Hemisphere and by identifying the
87 dominant mechanisms controlling the relationship between TSOS and growth for several regions with
88 contrasting climates (northern Asia, northern Europe, Central Europe, the Mediterranean region, the
89 western and eastern coast of the US, and the Colorado and Tibetan Plateaus) with different forest biomes
90 (boreal, Mediterranean, temperate, semi-arid and dry subalpine forests). We tested the hypothesis that the
91 shift of TSOS influences tree growth by changing its timing, duration, and rate according to the influence
92 of climate on the processes of xylem formation^{35, 39, 40}. We assumed that a shift of TSOS would lengthen
93 the growing season by modifying growing degree days and the availability of soil moisture and that such

94 phenological changes could affect growth through various ecophysiological mechanisms depending on the
95 ambient climatic conditions.

96

97 **Results**

98 **Response of tree growth to TSOS changes**

99 Most areas in the extratropical Northern Hemisphere had trends toward an earlier TSOS between 1948 and
100 2016. Correlation results show that 36.5% of these areas exhibited significant ($p < 0.05$ in a two-tailed
101 Student *t*-test) and 49.2% at least marginally significant ($p < 0.1$) advancing trends (Extended Data Fig. 1).
102 11.4% of the RWI chronologies had significant ($p < 0.05$, *t*-test) and 18.0% at least marginally significant
103 ($p < 0.1$) simple correlations with TSOS, and 7.7% had significant and 13.6% at least marginally significant
104 partial correlations (Extended Data Fig. 1). The correlations revealed distinct spatial patterns after gridding
105 onto a $2^\circ \times 2^\circ$ raster (Fig. 1). The area with negative TSOS-RWI correlations was generally larger than the
106 area with positive correlations (56% vs 33% in the simple correlation analyses and 46% vs 36% in the
107 partial correlation analyses; see histograms in Fig. 1C, D). Negative correlations dominated at high
108 latitudes ($>60^\circ\text{N}$), central Europe, eastern and western coastal North America, indicating that the advancing
109 TSOS could benefit tree growth in these regions. Correlations were mainly positive for the Colorado and
110 Tibetan Plateaus, indicating that an advance in TSOS could reduce growth in these regions. Similar patterns
111 were found for both the simple and partial correlations.

112 We calculated the 30-year (1969-1998) mean growing degree days (GST) and the 30-year mean
113 growing-season precipitation (GSP) to compare the ambient climatic characteristics of the RWI sites with
114 contrasting responses to changes in TSOS. GST for the RWI chronologies with significant negative TSOS
115 correlations was distinctly lower than for RWI chronologies with positive correlations (Fig. 1E, F). Linear
116 regression analyses of GST and GSP further indicated a higher regression coefficient for RWI chronologies
117 with significant negative correlations than for RWI chronologies with positive correlations. These results
118 suggest that the advance in TSOS would likely benefit tree growth in cold areas with a lower number of
119 GST and/or a higher GSP:GST ratio.

120 **Relationships between TSOS and RWI in climatically distinct regions**

121 We conducted path analyses to decompose the effect of TSOS on RWI, so that the magnitude of the
122 underlying processes responsible for the emergent correlations could be compared. TSOS-RWI
123 relationships of each tree-ring chronology involved in path analyses for the eight selected regions (northern
124 Asia, northern Europe, Central Europe, the Mediterranean region, the western and eastern coast of the US,
125 the Colorado Plateau and the Tibetan Plateau) are shown in Extended Data Fig. 2. The path diagram was
126 reliable in all regions; the specific model fits for each region are presented in Supplementary Table 1. The
127 path effects showed distinct responses between regions (Fig. 2). TSOS had a negative total effect on RWI
128 (i.e., higher RWI under advanced TSOS) for boreal forests in northern Asia and Europe, temperate forests
129 in central Europe and the east coast of the US, and for forests in the Mediterranean region and along the
130 west coast of the US. In boreal forests, the most pronounced pathway affecting RWI is the “growing degree
131 days (GDD) effect” (i.e., the path effect through the “TSOS—GDD—RWI” path), suggesting that an
132 advance in TSOS increases tree growth mainly through the increase in GDD. TSOS also had a negative
133 total effect on RWI in temperate and seasonally dry Mediterranean forests, but the path effect was stronger
134 through the length of the thermal growing season (GSL) than GDD, suggesting that the beneficial effect of
135 an advanced TSOS on growth was due to the extension of the thermal growing season, without a clear
136 effect of drought due to reduced SM. In contrast, TSOS for semi-arid forests on the Colorado Plateau had a
137 strong positive total effect on RWI (i.e., lower RWI under advanced TSOS). The positive effect through
138 GSL combined with the effect through GDD and SM, suggests that an advance in TSOS could reduce tree
139 growth due to the longer growing season, the increase in GDD, and the decrease in SM (soil drought)
140 caused by the increased GDD. TSOS for dry subalpine forests on the Tibetan Plateau also had a positive
141 effect on RWI, with the main path through changes to GSL, suggesting that the unfavorable situation of an
142 advanced TSOS for growth was mainly caused by the lengthening of the growing season.

143

144 **Discussion**

145 Our study has demonstrated that spatiotemporal shifts in TSOS can significantly and variably affect
146 tree growth in the extratropical Northern Hemisphere. This conclusion is supported by our current
147 understanding of the physiological mechanisms that underlie wood formation. As shown by xylogenetic

148 studies, wood formation involves sequential processes of cambial cell division, cell enlargement and cell-
149 wall thickening⁴¹. The onset of wood formation is the main factor that directly or indirectly triggers all
150 subsequent phases of xylem maturation³⁹. Small changes in the period of cell division can lead to
151 substantial increases in xylem cell production and growth⁴⁰. The rate of increase in xylem size peaks when
152 the cambium is dividing vigorously and most cells are undergoing the enlarging phase. These physiological
153 processes culminate at the end of spring and slow down in late summer and autumn when the tree ring is
154 almost fully formed^{38, 41, 42}. Therefore, tree growth would be enhanced by an earlier onset and also by
155 higher growth rates during the peak growing season in cold climates. Recent xylogenetic studies have also
156 demonstrated that a longer growing season induced by its earlier start will not benefit xylem formation in
157 trees located in drought-prone environments. Instead, warming induced drought could limit carbon
158 sequestration by reducing the rate of cell production^{35, 37}. Based on these physiological mechanisms, we
159 assumed that growth changes caused by shifts in TSOS can be inferred from tree-ring data.

160 Our results revealed a clear spatial pattern in the response of tree growth (RWI) to TSOS (Fig. 1).
161 Areas with beneficial effects of TSOS on RWI (i.e., negative correlation) are generally located in high-
162 latitude (above 60°N), Europe, as well as in eastern and western coastal North America. These cold and
163 humid regions have no or minimal water limitation during the growing season. This spatial distribution
164 generally agrees with the distribution of areas that exhibit a clear advance in the timing of foliar onset and
165 peak photosynthetic activity^{11, 19, 43}. This importantly suggests that enhanced carbon uptake induced by the
166 advance of TSOS promoted the production and accumulation of photosynthates and thus increased the
167 availability of resources for tree growth. Although a warmer autumn may offset the increased productivity
168 during spring due to a disproportionally larger increase in respiration compared with photosynthesis^{23, 24, 26}
169 and can additionally cause earlier foliar senescence⁴⁴, this is likely to affect carbon stored in pools with a
170 faster turnover rate such as shoots and leaves. However, the effect of autumnal warming was marginal for
171 “slow carbon”, i.e., that sequestered in the wood, compared to this canopy activity. The regions with
172 negative effects of TSOS on growth (i.e., positive correlation) were mainly located on the Colorado Plateau
173 and the Tibetan Plateau, corresponding to cold-dry conditions where forests are typically co-limited by the
174 availability of soil water and nutrients. Radial growth is more sensitive to low temperatures or drought than

175 photosynthesis⁴⁵ and may cease long before carbon uptake in response to water shortage⁴⁶. Warming during
176 the growing season in these regions may intensify drought, inhibit woody tissue formation^{37, 45}, and reverse
177 the positive effects of temperature on growth even in cold areas⁴⁷. An extended growing season may also
178 increase the risk of tree exposure to low temperature events such as spring frosts⁴⁸. These effects are possible
179 causes of reduced tree growth and constrain carbon accumulation in the wood.

180 The shift in the timing of TSOS may have affected GSL, GDD and SM. The change of GSL would
181 extend the time when cambial activity and wood formation are possible. In contrast, the change of GDD
182 and SM would affect growth rates^{35, 49}. All these factors can interact to modulate tree growth and the
183 resulting sequestration of carbon. Decomposing the effect of TSOS on radial growth in different forest
184 biomes – as we have done in this study – can therefore help advance our understanding of the effects of
185 TSOS on carbon sequestration and wood formation, and pave the way for improved forecasting of forest
186 carbon cycling.

187 The advance of TSOS benefited tree growth in the boreal forests of northern Asia and Europe, and the
188 path analyses indicated that the “GDD effect” was the primary responsible pathway (Fig. 2A). Our results
189 are consistent with previous studies of canopy processes reporting that an increase in vegetation greenness
190 was more pronounced across boreal ecosystems than in other regions⁵⁰, which was mainly due to the
191 alleviation of the limitation of cold temperatures on vegetation growth under climatic warming^{51, 52}. The
192 advance of TSOS also benefited tree growth in temperate forests of central Europe and the east coast of the
193 US, and Mediterranean forests of the Mediterranean region and the west coast of the US. The “GSL effect”
194 was the primary path effect in those areas (Fig. 2B). In central Europe and along the east coast of the US,
195 precipitation is adequate to abundant, and the summers are generally warm and humid. A lengthened GSL
196 extends the growth duration and favors tree growth there. The Mediterranean climate is characterized by
197 dry and hot summers, with optimal conditions for vegetation growth occurring during the cool and rainy
198 springs and autumns, often leading to a bimodal pattern of growth with a temporary cessation of growth in
199 summer⁵³. Photoperiods are longer in spring than in autumn, and an earlier reactivation of the cambium
200 after winter dormancy can harness this period for increasing production. A lengthening of the growing
201 season through the advance of TSOS may therefore benefit tree growth if spring droughts are not persistent

202 or severe. SM at the beginning of the growing season is also a major factor affecting tree radial growth^{54, 55},
203 but the advanced TSOS in our study may have had a limited effect on RWI via the “SM effects” (i.e. the
204 path effect through the “TSOS—GSL—GDD—SM—RWI” and “TSOS—SM—RWI” paths) in these
205 regions. The thermal conditions at the beginning of the growing season were mild and may not have caused
206 a severe loss of soil water through evaporation, but an advanced TSOS may accelerate snow melt and
207 increase the availability of soil water⁵⁶. These remaining uncertainties need to be comprehensively
208 addressed in future studies. The path effects of northern and central Europe are small compared with other
209 regions, perhaps due to the difference in the distance from the ocean and the complexity in topography and
210 species composition, which also need to be studied with more detail in future work.

211 The advance of TSOS negatively affected growth in semi-arid forests on the Colorado Plateau and dry
212 subalpine forests on the Tibetan Plateau. Path analysis further indicated that growth reductions under
213 advanced TSOS were primarily caused by the “GSL effect” (Fig. 2). This result was not consistent with our
214 original hypothesis in the path diagram that an extended GSL would enhance tree radial growth
215 (Supplementary Fig. 1) and may involve more complex mechanisms. Extended GSL in these regions,
216 combined with higher heat accumulation (“GDD effect”) and/or evapotranspiration of soil water (i.e., the
217 path effect through the “TSOS—GSL—GDD—SM—RWI”), may induce both atmospheric and soil
218 droughts. Droughts will trigger stomatal closure, increase water tension in the xylem, and deplete the
219 contents of nonstructural carbohydrates in trees⁵⁷⁻⁵⁹, thus reducing the rate of wood production³⁵. Forests in
220 these regions also suffered more from frost days than those in high latitude regions (see Supplementary Fig.
221 2). Earlier TSOS may increase tree exposure to spring frost and thereby reduce tree growth^{48, 60}. The
222 specific mechanisms underlying these processes need to be addressed in further experimental studies.

223 Uncertainties in our analyses were mainly introduced by three sources: the spatial representativeness
224 of the tree-ring series, the determination of the TSOS thresholds and the establishment of the path diagram.
225 The ITRDB data set contains a large imbalance in the spatial distribution of sites and in its species
226 composition^{61, 62}. Further, the local microenvironment, stand structure, or biotic and abiotic disturbances are
227 often unknown but can also impact tree radial growth and phenological responses^{10, 63, 64}. To mitigate
228 potential biases associated with these caveats, we first gridded the correlation coefficients and then

229 displayed the percentage of the direction instead of the magnitude of the correlation coefficients. We were
230 thereby able to extract the dominant spatial patterns of the response of tree growth to shifts in the timing of
231 the thermal growing season.

232 The thermal threshold for growth of 5 °C is widely accepted and used⁶, but debatable because the
233 choice of threshold may lead to different conclusions⁴. A more vegetative based threshold (for instance the
234 threshold from vegetation greenness) is, however, difficult to achieve due to the inconsistency in temporal
235 availability of tree-ring data and satellite-retrieved observations⁶². Biological evidence suggests that the
236 daily mean temperature threshold for the onset of xylem growth in conifers at high altitudes and in cold
237 climates is 5.6 to 8.0 °C^{32, 65}. The critical threshold of mean air temperature at alpine treelines is about 3.9
238 °C³¹. With these premises, we assumed the threshold for TSOS and GDD range between 4 to 6 °C while
239 exploring the response of tree growth to TSOS at large-spatial scales and chose to present the results for the
240 5 °C cutoff. Reassuringly, the results of analyses with other cutoffs showed similar patterns, confirming the
241 robustness of the results.

242 The establishment of our path diagram was based on experimental studies; advanced TSOS would
243 extend growth duration (indicated by GSL) and affect growth rates (controlled by GDD and SM), thus
244 influencing annual tree growth. Path analysis is an extension of multiple linear regression. We therefore
245 assumed that the relationships among the variables were mainly linear, which is not always consistent with
246 our current understanding of the complex responses of tree growth to climate⁶⁶⁻⁶⁸. Encouragingly, the
247 relationships between TSOS and RWI in the eight regions were mostly linear (Extended Data Fig. 2). We
248 therefore considered our use of path analyses to be appropriate.

249 We found that the impact of shifts in the timing and duration of the thermal growing season could be
250 detected in tree rings at regional to hemispheric scales. Our study thus allows for the further exploration of
251 the impact of climatic trends and variability on tree growth. Such information is essential for integrating
252 information regarding the responses of foliage and stems to climate change, and for predicting future
253 vegetation performance. Explaining the influence of plant phenology on carbon sequestration solely based
254 on the perspective of foliar phenology and photosynthesis seasonality (which drive carbon uptake) is
255 insufficient. Low temperatures and drought constrain growth more than photosynthesis⁴⁵. A carbon sink

256 (i.e., wood) oriented view on phenological impacts is therefore essential for predicting carbon sequestration
257 capacity, because wood is the primary long-term carbon storage pool in forests. Wood formation, however,
258 is notoriously difficult to quantify using satellite observations or techniques of eddy covariance⁴¹. Our
259 study implies that the analysis of tree rings at regional to global scales could provide new solutions to
260 differentiate between shifts in the turnover of “slow” and “fast” carbon pools under a rapidly changing
261 climate⁶⁹.

262 In summary, our study provides strong evidence that shifts in TSOS influence tree radial growth in the
263 extratropical Northern Hemisphere. The advance of TSOS is more likely to enhance tree growth in cold
264 humid areas with a higher water:heat ratio, whereas growth in cold dry areas may be reduced. Our results
265 also indicated that the primary path effect of TSOS on growth differed among forest biomes. The beneficial
266 effects in the boreal forests of northern Asia and Europe were mainly due to the alleviation of thermal
267 limitation on wood formation, so that higher growth rates were possible, but the primary beneficial effect in
268 the temperate forests of central Europe and the east coast of the US and Mediterranean forests involved a
269 lengthening of the growing season. The negative effects for semi-arid and dry alpine forests on the cold dry
270 Colorado Plateau and the Tibetan Plateau were primarily due to a longer period of growth, presumably due
271 to associated droughts driven by heat, as well as by an increased likelihood of spring frosts. This study
272 reveals how climate affects tree growth through wood phenology and contributes to improving our ability
273 to predict trends in the capacity of forests to sequester carbon at regional to global scales.

274

275 **Methods**

276 **Experimental design**

277 We raised fundamental but still unresolved questions of whether and how the advance of the thermal
278 growing season in spring influences tree growth across environmental gradients. We addressed these
279 questions by investigating the relationships between TSOS and tree radial growth across the extratropical
280 Northern Hemisphere with correlation analyses and by identifying the dominant mechanisms controlling
281 the relationships in path analyses for several regions with contrasting climates. A total of 3451 tree-ring
282 width chronologies and daily climatic data for 1948-2014 were used to conduct these analyses.

283 **Data**

284 **Tree-ring width chronologies**

285 Raw tree-ring width chronologies from 4219 sites across the extratropical Northern Hemisphere (20-75°N)
286 were selected from the reformatted data set of the International Tree-Ring Data Bank (ITRDB)⁶¹, as well as
287 83 sites on the Tibetan Plateau (Supplementary Table 2) from the tree-ring group of the Institute of Tibetan
288 Plateau Research Chinese Academy of Sciences (ITPCAS) (<https://doi.org/10.11888/Terre.tpd.271925>).
289 We excluded chronologies shorter than 30 years after 1948 and those where TSOS varied little (i.e. no
290 change of TSOS for >20 years), for a total of 3451 sites retained for further analyses. Of these
291 chronologies, 73.6% (2540) were from evergreen conifers, 9.1% (314) from deciduous conifers (mainly
292 larch), 16.5% (569) from broadleaf species, and 0.2% (7) from shrubs at the boreal treeline. Twenty-one
293 chronologies lacked information about tree species. To transform the tree-ring width data into a ring-width
294 index (RWI) that accentuates the variability of annual to decadal growth, we removed long-term trends
295 caused by aging and increasing trunk diameter by fitting either a negative exponential curve or a cubic
296 smoothing spline (removing 50% of the variance for a period of 67% of series length) to the raw ring-width
297 series using the dplr package (version 1.7.1)⁷⁰ in R⁷¹. Mean site chronologies of RWI after 1948 were
298 calculated using bi-weight robust means.

299

300 **Climatic and soil-moisture data**

301 Daily grids of mean air temperature and total precipitation for 1948 to 2016 were obtained from the Global
302 Meteorological Forcing Dataset of the Terrestrial Hydrology Research Group at Princeton University
303 (<http://hydrology.princeton.edu/data.pgf.php>) at a spatial resolution of 0.25°⁷². Daily soil-moisture content
304 (SM) in the root zone (0-100 cm) was obtained from the NASA Global Land Data Assimilation System
305 Version 2 (GLDAS-2)
306 (https://disc.gsfc.nasa.gov/datasets/GLDAS_CLSM025_D_2.0/summary?keywords=GLDAS2.0) at a
307 resolution of 0.25°. GLDAS-2 is forced entirely with the Princeton meteorological forcing input data and
308 provides a temporally consistent series from 1948 to 2014.

309 We extracted the timing and length of the thermal growing season for each year based on daily mean
310 air temperature. TSOS was defined as the first six uninterrupted days with daily mean temperatures $>5^{\circ}\text{C}$
311 at mid and high latitudes⁷³. The end of the thermal growing season (TEOS) was defined as the first six
312 uninterrupted days after 1 July with daily mean temperatures $<5^{\circ}\text{C}$. GSL was calculated as the time
313 between TSOS and TEOS.

314 Growing degree days (GDD), which represent the effective accumulation of heat for vegetation
315 growth during the growing season, were calculated as the sum of daily mean temperatures $>5^{\circ}\text{C}$ ⁵⁴:

$$316 \quad GDD = \sum_{TSOS}^{TEOS} (T_i - 5) \text{ if } T_i > 5 \quad (1)$$

317 where T_i is the mean temperature on day i .

318 Growing-season precipitation was calculated as the sum of daily precipitation during the thermal growing
319 season. Mean SM during the growing season was the average of the daily content in the root zone during
320 the thermal growing season. The 30-year mean GDD (GST) and the 30-year mean growing-season
321 precipitation (GSP) were calculated for 1969-1998. When choosing an aridity metric for our study, we
322 decided to use a simple index that relies only on the most widely measured variables: temperature and
323 precipitation. We favored the GSP:GST ratio (similar to the Selyaninov hydrothermic coefficient⁷⁴) over
324 more complex indices because the latter often require input variables that are best measured locally. These
325 include atmospheric or even soil moisture content, which are not ubiquitously available in remote areas to
326 feed the data pipelines that produce global gridded climate products. We thus deemed the GSP:GST ratio to
327 be a robust, reliable and well-established aridity metric for our study. It was used to compare aridity
328 condition during the growing season among tree-ring sites.

329

330 **Analyses**

331 **Correlations**

332 We calculated both simple and partial Pearson correlations to explore the effects of TSOS on tree growth
333 for each site of tree-ring chronology. We eliminated the effects of GSL, GDD and SM when calculating
334 partial correlation coefficients between TSOS and RWI. Tree-ring width chronologies are likely co-driven
335 by local site factors such as microclimatic and soil conditions, forest composition and competition in

336 closed-canopy stands and a possible mismatch between the site location and the gridded climatic data (e.g.
337 elevation). To reduce the impact of these site-specific factors and identify general spatial pattern in the
338 correlation coefficients, we gridded the correlation coefficients by $2^{\circ} \times 2^{\circ}$ and displayed the percentage of
339 tree-ring series with positive coefficients within each grid.

340

341 **Path analysis**

342 Path analysis is an extension of multiple regression analyses used to evaluate causal models by examining
343 the linear relationships between independent and dependent variables⁷⁵. Path analysis decomposes bivariate
344 correlation coefficients into path coefficients, which represent the relative importance of prespecified
345 hypotheses within the same path diagram. We used the existing information of how TSOS affects RWI (see
346 the Introduction section) to test a path diagram containing four hypothetical associations (Supplementary
347 Fig. 1). First, the advance in TSOS would extend GSL and thereby enhance tree radial growth (represented
348 by RWI). Second, the advance in TSOS would extend GSL and increase GDD, causing a positive change in
349 RWI. Third, the advance in TSOS would extend GSL, increase GDD and lead to a shortage of soil
350 moisture, with negative effects on RWI. Fourth, the change in TSOS could affect SM by accelerating snow
351 melt, by increasing the thawing of permafrost or by changing the proportion of precipitation during the
352 growing season⁵⁶, thereby promoting tree growth and increasing RWI.

353 We used the “sem” package (version 3.1.9)⁷⁶ in R to calculate the standardized path coefficients of the
354 preset path diagram. Path effects were then calculated as the product of the standardized path coefficients
355 along each pathway. We compared the bivariate correlation coefficients (i.e. TSOS and RWI) and the total
356 path effects (i.e. the sum of the four path effects) of all 3451 RWI series to determine the fit of the preset
357 path diagram to our data. The relationships between the bivariate correlation coefficients and the total path
358 effects were consistent (Supplementary Fig. 3).

359 We selected eight regions based on the spatial patterns identified by the correlation analyses and
360 climatological consistency to examine the general characteristics of the path effects. The definition of
361 northern Asia and Europe, central Europe, the Mediterranean region and the Tibetan Plateau referred to
362 IPCC climate reference regions⁷⁷, the west and east coast of the US and the Colorado Plateau referred the

363 hydrologic and geographic unit. For the eight regions, general climatic conditions were presented in
364 Supplementary Fig. 4 and forest conditions were described in the supplementary text. Because we aimed to
365 decompose correlations into different processes for the interpretation of underlying mechanisms, only RWI
366 chronologies with at least marginally significant correlations ($p < 0.1$) were included in the regional path
367 analyses⁵⁶. Anomalies of climatic variables (i.e., TSOS, GSL, GDD and SM) were calculated for each RWI
368 chronology in reference to its 30-year (1969-1998) mean climate condition. Then we used RWIs and their
369 corresponding climatic anomalies within the same region to conduct the path analysis. All variables were
370 standardized prior to path analyses. Many fitting measures can appraise a path diagram. We measured the
371 adequacy of the fitness of the path diagram in each region using the following criteria: goodness-of-fit
372 index (GFI) ≥ 0.95 , comparative fit index (CFI) ≥ 0.90 , root mean square error of approximation (RMSEA)
373 ≤ 0.10 , nonnormed fit index (NNFI) ≥ 0.92 and standardized root mean square residual (SRMR) ≤ 0.08 .
374 The path diagram was considered reliable when three of these five criteria were met⁷⁸.

375

376 **Results validation**

377 In order to confirm the robustness of our results, we tested different thresholds of TSOS, as well as of GDD
378 at 4, 4.5, 5.5 and 6 °C, and conducted the full analysis for each of them. The results showed similar pattern
379 and are presented in the Supplementary Table 3.

380

381 **Data availability**

382 The reformatted data set of the International Tree-Ring Data Bank were obtained from
383 <https://doi.org/10.5061/dryad.kh0qh06>. Tree-ring width data from the ITPCAS tree-ring group are available
384 from <https://doi.org/10.11888/Terre.tpd.271925>. The Global Meteorological Forcing Dataset of the
385 Terrestrial Hydrology Research Group at Princeton University were obtained from
386 <http://hydrology.princeton.edu/data.pgf.php>. The NASA Global Land Data Assimilation System Version 2
387 were obtained from
388 https://disc.gsfc.nasa.gov/datasets/GLDAS_CLSM025_D_2.0/summary?keywords=GLDAS2.0.

389

390

391 **Code availability**

392 Statistical analysis in this study were performed with publicly available packages in R (version 3.6.2, dplR
393 and sem packages) and Python (version 3.8, scipy package), and the figures were produced using Python
394 (matplotlib, cartopy and seaborn packages). The custom code for the analysis of the data are available from
395 <https://doi.org/10.11888/Terre.tpdc.271925>.

396

397 **Acknowledgments**

398 We acknowledge all contributors to the International Tree-Ring Databank for providing tree-ring data. This
399 study was supported by the Second Tibetan Plateau Scientific Expedition and Research Program (STEP)
400 (2019QZKK0301), the National Natural Science Foundation of China (41907387, 42030508, 41988101)
401 and the China Postdoctoral Science Foundation (2019M660813). JP was funded by Spanish Government
402 projects PID2019-110521GB-I00, Fundación Ramón Areces project ELEMENTAL-CLIMATE, and
403 Catalan government project SGR2017-1005.

404

405 **Author Contributions Statement**

406 S.G. and E.L. designed the research, S.G. and R.L. performed the analysis and S.G. drafted the manuscript.
407 E.L., F.B., J.J.C., Y.H.F., S.P., S.R., M.S., T.W. and J.P. contributed ideas, interpreted the results and were
408 involved in the editing and writing of the manuscript.

409

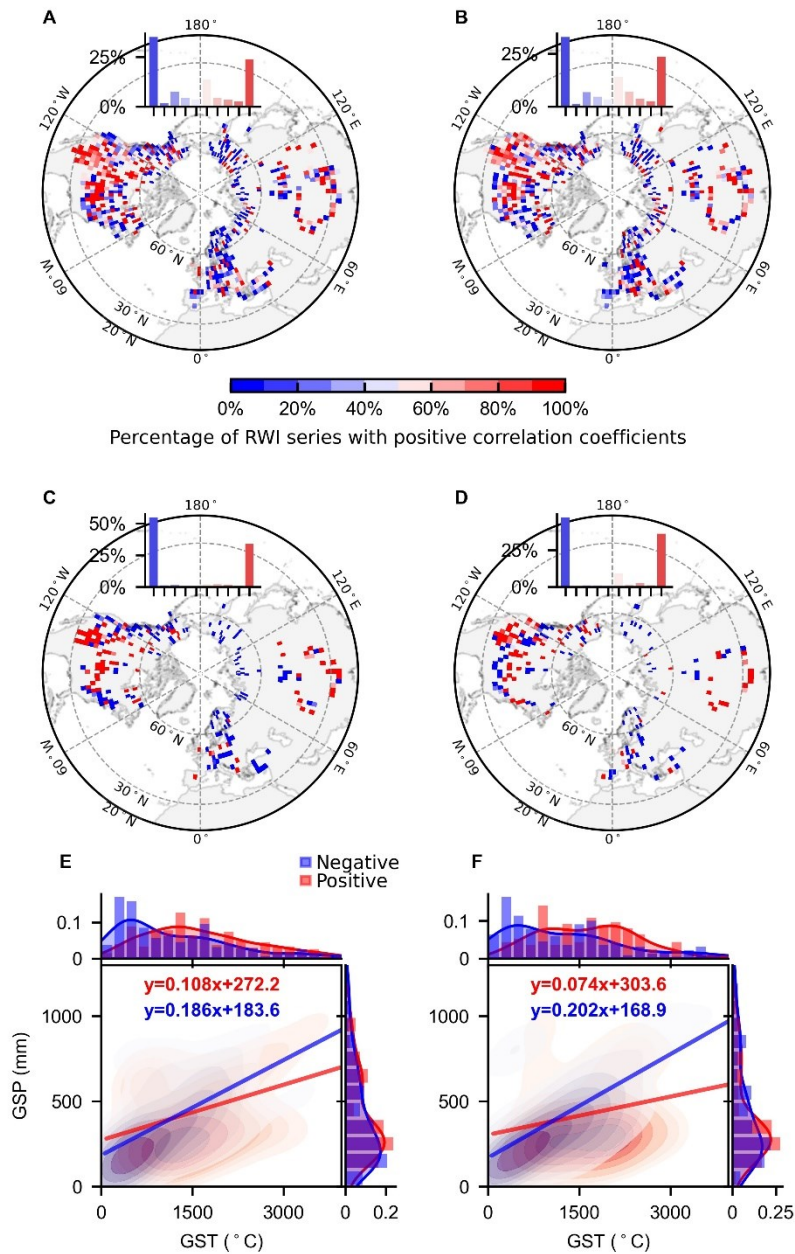
410 **Competing Interest Statement**

411 The authors declare no conflicts of interest.

412

413

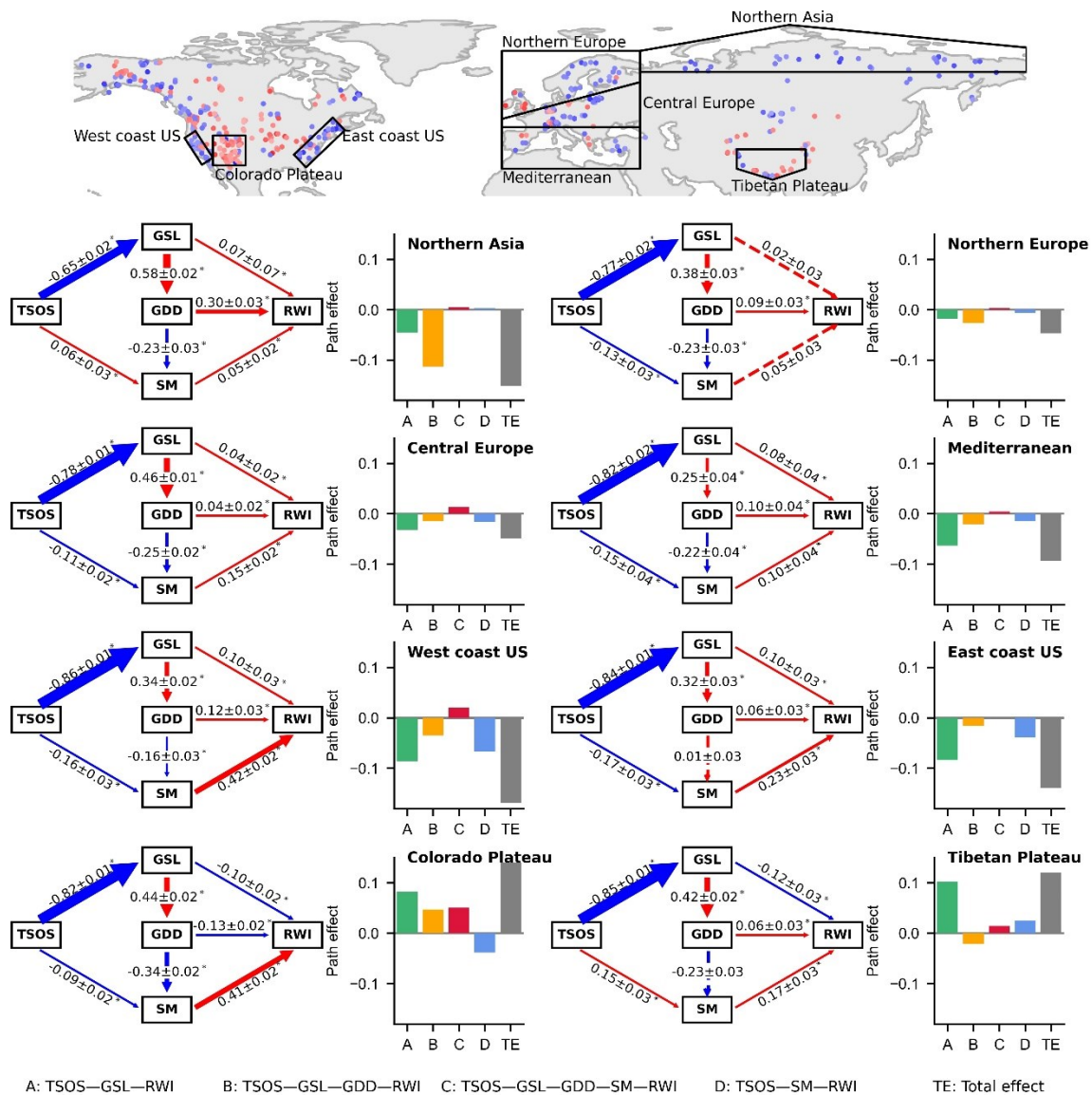
414



415

416 **Fig. 1 | Responses of tree growth to changes in the onset of the thermal growing season (TSOS) across**
 417 **the extratropical Northern Hemisphere.** Spatial patterns of the percentage of tree-ring series (represented
 418 by RWI) with a positive simple correlation coefficient (A), partial correlation coefficient (B), significant (p
 419 < 0.1) simple correlation coefficient (C) and significant partial correlation coefficient (D) between RWI
 420 and TSOS within $2^\circ \times 2^\circ$ grids. The number of tree-ring width chronologies considered in each grid are
 421 presented in Supplementary Fig. 5. The histograms in panels (A) to (D) present the frequency distributions

422 of the percentages. Climatic characteristics of tree-ring sites with a significant simple correlation
423 coefficient (**E**) and partial correlation coefficient (**F**) in the space of GST and GSP. The histograms located
424 at the top and right of panels (**E**) and (**F**) present the distributions of the tree-ring sites along the GST and
425 GSP gradients. The blue and red kernel density plots and histograms represent tree-ring chronologies with
426 negative and positive correlation coefficients, respectively. The lines in panels (**E**) and (**F**) are derived from
427 linear regression, the shown regression equations are all significant ($p < 0.001$) estimated using the *F*-test.
428



429

430 **Fig. 2 | Path diagrams and path effects for northern Asia, northern and central Europe, the**

431 **Mediterranean region, the west and east coasts of the US, the Colorado Plateau, and the Tibetan**

432 **Plateau.** In the geographic map, dots represent the location of tree-ring chronologies with significant ($p <$

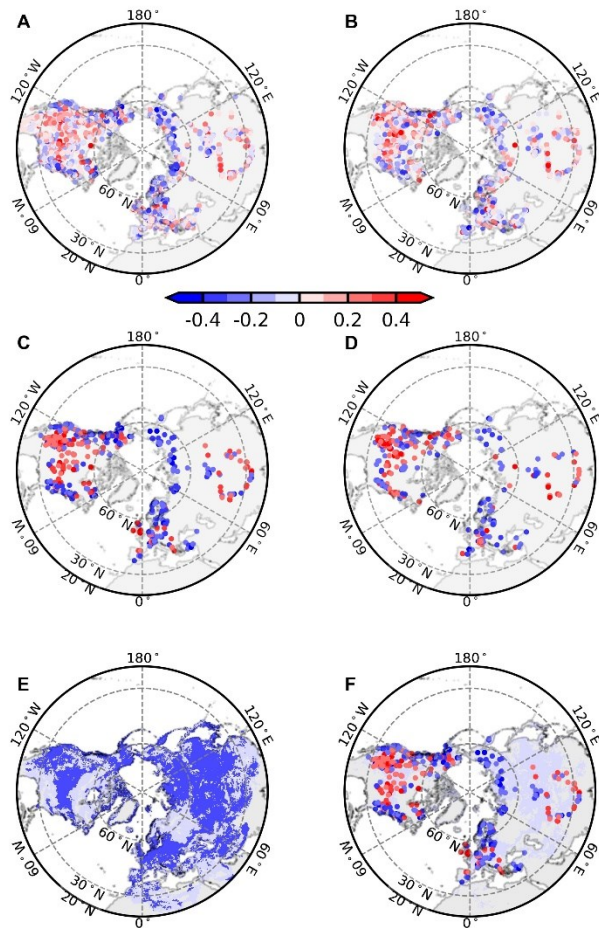
433 0.1) positive (red dots) and negative (blue dots) simple correlation with TSOS; boxes delineate the eight

434 regions. The numbers in the path diagrams represent the mean and standard error of standardized path

435 coefficients in the regions, asterisks indicate the significance of the path coefficients ($p < 0.05$) and the

436 colors (negative and positive effects are presented as blue and red arrows, respectively) and widths of the

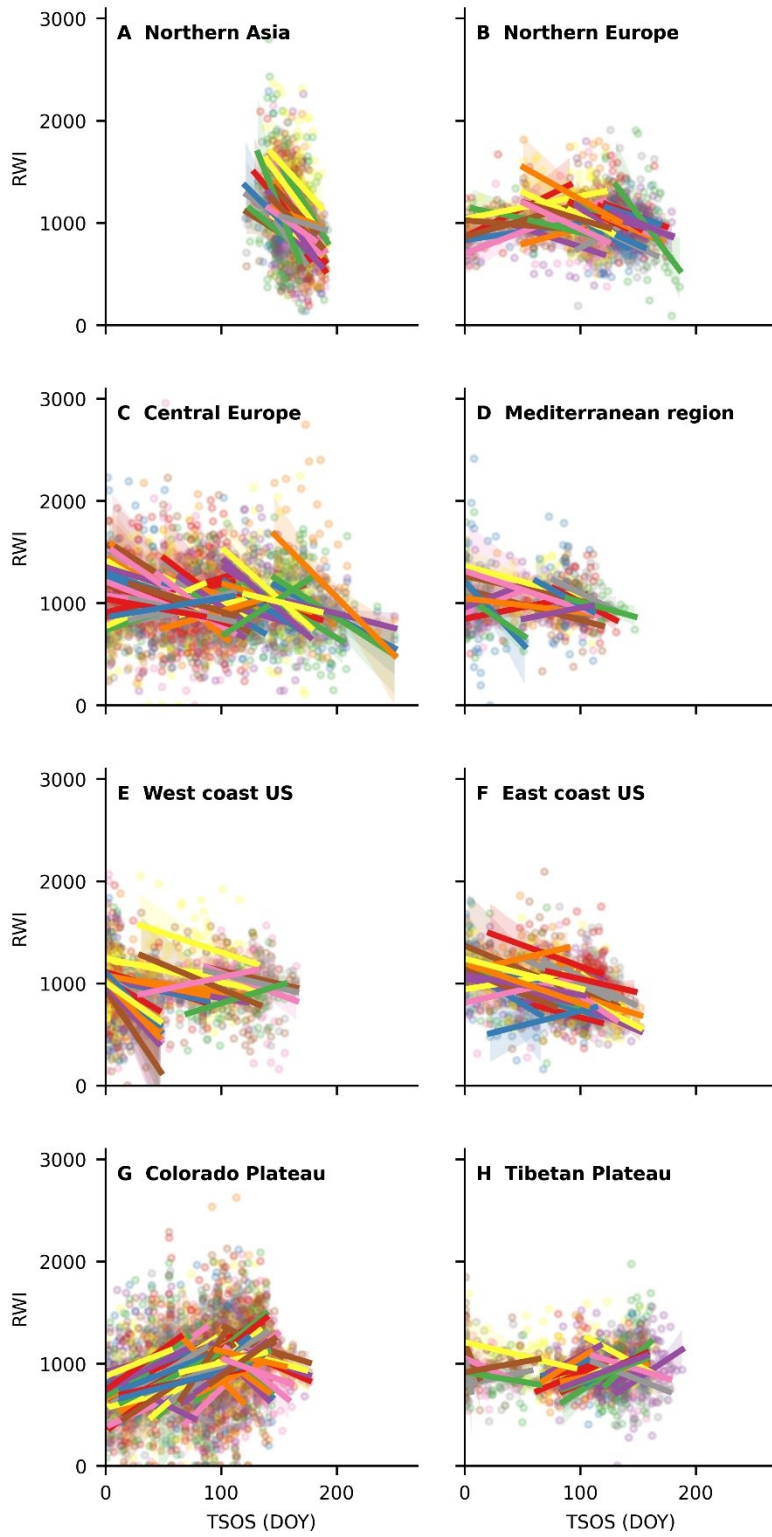
437 arrows represent the signs and magnitudes of the path coefficients, respectively. A, B, C and D in the
438 panels on the right represent the effect of four major paths, TE represents the total effect. The number of
439 tree-ring width chronologies for each region is presented in Supplementary Fig. 6.



440

441 **Extended Data Fig. 1|Responses of tree growth to changes in TSOS in the extratropical Northern**
 442 **Hemisphere.** Spatial distributions of simple correlation coefficients (A), partial correlation coefficients
 443 (B), significant ($p < 0.1$) simple correlation coefficients (C) and significant ($p < 0.1$) partial correlation
 444 coefficients (D) of TSOS and RWI. (E) Areas with significant ($p < 0.1$, dark blue) and nonsignificant (light
 445 blue) trends toward earlier TSOS between 1948 and 2016 in the extratropical Northern Hemisphere. (F)
 446 Areas with significant ($p < 0.05$, blue shaded area) trends toward earlier TSOS overlapping tree-ring
 447 chronologies with significant ($p < 0.1$) simple correlation coefficients of TSOS and RWI. The significance
 448 of the correlation analyses is estimated by two-tailed Student's t -test. This figure was generated using the
 449 matplotlib and cartopy package in Python.

450



452 **Extended Data Fig. 2 | Scatter plots of TSOS-RWI relationships in different regions.** TSOS-RWI
453 relationships of tree-ring chronologies with significant ($p < 0.1$) simple correlations for northern Asia (A),
454 northern Europe (B), central Europe (C), the Mediterranean region (D), the west coast of the US (E), the
455 east coast of the US (F), the Colorado Plateau (G) and the Tibetan Plateau (H). The predicted mean (solid
456 lines) is bounded by the 95% confidence intervals (shaded areas). This figure was generated using the
457 seaborn package, “lplot” function in Python.
458

459

460 **References**

- 461 1. K. E. Trenberth, P. D. Jones, Observations: Surface and atmospheric climate change, in Climate
462 change 2007: the physical science basis: contribution of working group I to the fourth assessment
463 report of the intergovernmental panel on climate change, (Cambridge Univ. Press, 2007), pp. 235–335.
- 464 2. H. W. Linderholm, Growing season changes in the last century. *Agr. Forest Meteorol.* 137, 1–14
465 (2006).
- 466 3. B. Yang, M. He, V. Shishov, I. Tychkov, E. Vaganov, S. Rossi, F.C. Ljungqvist, A. Bräuning, J.
467 Griebinger, New perspective on spring vegetation phenology and global climate change based on
468 Tibetan Plateau tree-ring data. *Proc. Natl. Acad. Sci. USA.* 114, 6966–6971 (2017).
- 469 4. M. Shen, Y. Tang, J. Chen, W. Yang, Specification of thermal growing season in temperate China
470 from 1960 to 2009. *Clim. Change.* 114, 783–798 (2012).
- 471 5. B. Zhou, P. Zhai, Y. Chen, R. Yu, Projected changes of thermal growing season over Northern Eurasia
472 in a 1.5°C and 2°C warming world. *Environ. Res. Lett.* 13, 35004 (2018).
- 473 6. J. Barichivich, K. R. Briffa, T. J. Osborn, T. M. Melvin, J. Caesar, Thermal growing season and
474 timing of biospheric carbon uptake across the Northern Hemisphere. *Global Biogeochem. Cycles.* 26,
475 B4015 (2012).
- 476 7. R. Buitenwerf, L. Rose, S. I. Higgins, Three decades of multi-dimensional change in global leaf
477 phenology. *Nat. Clim. Change.* 5, 364–368 (2015).
- 478 8. A. Gonsamo, J. M. Chen, Y. W. Ooi, Peak season plant activity shift towards spring is reflected by
479 increasing carbon uptake by extratropical ecosystems. *Global Change Biol.* 24, 2117–2128 (2018).
- 480 9. A. Menzel, T. H. Sparks, N. Estrella, E. Koch, A. Aasa, R. Ahas, K. Alm-Kübler, P. Bissolli, O.
481 Braslavská, A. Briede, F. M. Chmielewski, Z. Crepinsek, Y. Curnel, A. Dahl, C. Defila, A. Donnelly,
482 Y. Filella, K. Jatzcak, F. Mages, A. Mestre, Ø. Nordli, J. Peñuelas, P. Pirinen, V. Remišová, H.
483 Scheffinger, M. Striz, A. Susnik, A.J.H. Van Vliet, F. Wielgolaski, S. Zach, A. Zust, European
484 phenological response to climate change matches the warming pattern. *Global Change Biol.* 12, 1969–
485 1976 (2006).

- 486 10. R. A. Montgomery, K. E. Rice, A. Stefanski, R. L. Rich, P. B. Reich, Phenological responses of
487 temperate and boreal trees to warming depend on ambient spring temperatures, leaf habit, and
488 geographic range. *Proc. Natl. Acad. Sci. USA*. 117, 10397–10405 (2020).
- 489 11. S. Piao, J. Tan, A. Chen, Y. H. Fu, P. Ciais, Q. Liu, I.A. Janssens, S. Vicca, Z. Zeng, S. Jeong, Y. Li,
490 R.B. Myneni, S. Peng, M. Shen, J. Peñuelas, Leaf onset in the northern hemisphere triggered by
491 daytime temperature. *Nat. Commun.* 6, 6911 (2015).
- 492 12. J. Barichivich, K. R. Briffa, R. B. Myneni, T. J. Osborn, T. M. Melvin, P. Ciais, S. Piao, C. Tucker,
493 Large-scale variations in the vegetation growing season and annual cycle of atmospheric CO₂ at high
494 northern latitudes from 1950 to 2011. *Global Change Biol.* 19, 3167–3183 (2013).
- 495 13. J. Peñuelas, T. Rutishauser, I. Filella, Phenology Feedbacks on Climate Change. *Science*. 324, 887–
496 888 (2009).
- 497 14. S. Piao, Z. Liu, T. Wang, S. Peng, P. Ciais, M. Huang, A. Ahlstrom, J.F. Burkhart, F. Chevallier, I. A.
498 Janssens, S. Jeong, X. Lin, J. Mao, J. Miller, A. Mohammat, R. B. Myneni, J. Peñuelas, X. Shi, A.
499 Stohl, Y. Yao, Z. Zhu, P. P. Tans, Weakening temperature control on the interannual variations of
500 spring carbon uptake across northern lands. *Nat. Clim. Change*. 7, 359–363 (2017).
- 501 15. A. D. Richardson, T. A. Black, P. Ciais, N. Delbart, M. A. Friedl, N. Gobron, D. Y. Hollinger, W. L.
502 Kutsch, B. Longdoz, S. Luysaert, M. Migliavacca, L. Montagnani, J. W. Munger, E. Moors, S. Piao,
503 C. Rebmann, M. Reichstein, N. Saigusa, E. Tomelleri, R. Vargas, A. Varlagin, Influence of spring and
504 autumn phenological transitions on forest ecosystem productivity. *Philos. Trans. R. Soc., B*. 365,
505 3227–3246 (2010).
- 506 16. G. B. Bonan, Forests and Climate Change: Forcings, Feedbacks, and the Climate Benefits of Forests.
507 *Science*. 320, 1444–1449 (2008).
- 508 17. S. Piao, Q. Liu, A. Chen, I. A. Janssens, Y. Fu, J. Dai, L. Liu, X. Lian, M. Shen, X. Zhu, Plant
509 phenology and global climate change: Current progresses and challenges. *Global Change Biol.* 25,
510 1922–1940 (2019).

- 511 18. Y. H. Fu, H. Zhao, S. Piao, M. Peaucelle, S. Peng, G. Zhou, P. Ciais, M. Huang, A. Menzel, J.
512 Peñuelas, Y. Song, Y. Vitasse, Z. Zeng, I.A. Janssens, Declining global warming effects on the
513 phenology of spring leaf unfolding. *Nature*. 526, 104–107 (2015).
- 514 19. T. Park, C. Chen, M. M. Fauria, H. Tømmervik, S. Choi, A. Winkler, U. S. Bhatt, D. A. Walker, S.
515 Piao, V. Brovkin, R. R. Nemani, R. B. Myneni, Changes in timing of seasonal peak photosynthetic
516 activity in northern ecosystems. *Global Change Biol.* 25, 2382–2395 (2019).
- 517 20. C. Xu, H. Liu, A. P. Williams, Y. Yin, X. Wu, Trends toward an earlier peak of the growing season in
518 Northern Hemisphere mid-latitudes. *Global Change Biol.* 22, 2852–2860 (2016).
- 519 21. X. Wang, J. Xiao, X. Li, G. Cheng, M. Ma, G. Zhu, M. A. Arain, T. A. Black, R.S. Jassal, No trends
520 in spring and autumn phenology during the global warming hiatus. *Nat. Commun.* 10, 2389 (2019).
- 521 22. S. Piao, P. Friedlingstein, P. Ciais, N. Viovy, J. Demarty, Growing season extension and its impact on
522 terrestrial carbon cycle in the Northern Hemisphere over the past 2 decades. *Global Biogeochem.*
523 *Cycles*. 21, B3018 (2007).
- 524 23. W. Buermann, P. R. Bikash, M. Jung, D. H. Burn, M. Reichstein, Earlier springs decrease peak
525 summer productivity in North American boreal forests. *Environ. Res. Lett.* 8, 24027 (2013).
- 526 24. W. Buermann, M. Forkel, M. O Sullivan, S. Sitch, P. Friedlingstein, V. Haverd, A. K. Jain, E. Kato,
527 M. Kautz, S. Lienert, D. Lombardozzi, J. E. M. S. Nabel, H. Tian, A. J. Wiltshire, D. Zhu, W. K.
528 Smith, A. D. Richardson, Widespread seasonal compensation effects of spring warming on northern
529 plant productivity. *Nature*. 562, 110–114 (2018).
- 530 25. X. Lian, S. Piao, L. Z. X. Li, Y. Li, C. Huntingford, P. Ciais, A. Cescatti, I. A. Janssens, J. Peñuelas,
531 W. Buermann, A. Chen, X. Li, R. B. Myneni, X. Wang, Y. Wang, Y. Yang, Z. Zeng, Y. Zhang, T. R.
532 McVicar, Summer soil drying exacerbated by earlier spring greening of northern vegetation. *Sci. Adv.*
533 6, eaax0255 (2020).
- 534 26. S. Piao, P. Ciais, P. Friedlingstein, P. Peylin, M. Reichstein, S. Luyssaert, H. Margolis, J. Fang, A.
535 Barr, A. Chen, A. Grelle, D. Y. Hollinger, T. Laurila, A. Lindroth, A. D. Richardson, T. Vesala, Net
536 carbon dioxide losses of northern ecosystems in response to autumn warming. *Nature*. 451, 49–52
537 (2008).

- 538 27. H. Wang, H. Liu, G. Cao, Z. Ma, Y. Li, F. Zhang, X. Zhao, X. Zhao, L. Jiang, N. J. Sanders, A. T.
539 Classen, J. S. He, Alpine grassland plants grow earlier and faster but biomass remains unchanged over
540 35 years of climate change. *Ecol. Lett.* 23, 701–710 (2020).
- 541 28. Y. Pan, R. A. Birdsey, J. Fang, R. Houghton, P. E. Kauppi, W. A. Kurz, O. L. Phillips, A. Shvidenko,
542 S. L. Lewis, J. G. Canadell, P. Ciais, R. B. Jackson, S. W. Pacala, A. D. McGuire, S. Piao, A.
543 Rautiainen, S. Sitch, D. Hayes, A Large and Persistent Carbon Sink in the World's Forests. *Science*.
544 333, 988–993 (2011).
- 545 29. N. Delpierre, Y. Vitasse, I. Chuine, J. Guillemot, S. Bazot, T. Rutishauser, C. B. K. Rathgeber,
546 Temperate and boreal forest tree phenology: from organ-scale processes to terrestrial ecosystem
547 models. *Ann. Forest Sci.* 73, 5–25 (2016).
- 548 30. J. Huang, Q. Ma, S. Rossi, F. Biondi, A. Deslauriers, P. Fonti, E. Liang, H. Makinen, W. Oberhuber,
549 C. Rathgeber, R. Tognetti, V. Treml, B. Yang, J. L. Zhang, S. Antonucci, Y. Bergeron, J. J. Camarero,
550 F. Campelo, K. Cufar, H. E. Cuny, M. De Luis, A. Giovannelli, J. Gricar, A. Gruber, V. Gryc, A.
551 Guney, X. Guo, W. Huang, T. Jyske, J. Kaspar, G. King, C. Krause, A. Lemay, F. Liu, F. Lombardi,
552 D. C. E. Martinez, H. Morin, C. Nabais, P. Nojd, R. L. Peters, P. Prislan, A. Saracino, I. Swidrak, H.
553 Vavreik, J. Vieira, B. Yu, S. Zhang, Q. Zeng, Y. Zhang, E. Ziaco, Photoperiod and temperature as
554 dominant environmental drivers triggering secondary growth resumption in Northern Hemisphere
555 conifers. *Proc. Natl. Acad. Sci. USA.* 117, 20645–20652 (2020).
- 556 31. X. Li, E. Liang, J. Gričar, S. Rossi, K. Čufar, A. M. Ellison, Critical minimum temperature limits
557 xylogenesis and maintains treelines on the southeastern Tibetan Plateau. *Sci. Bull.* 62, 804–812
558 (2017).
- 559 32. S. Rossi, A. Deslauriers, J. Gričar, J. Seo, C. B. Rathgeber, T. Anfodillo, H. Morin, T. Levanic, P.
560 Oven, R. Jalkanen, Critical temperatures for xylogenesis in conifers of cold climates. *Global Ecol.*
561 *Biogeogr.* 17, 696–707 (2008).
- 562 33. A. Lenz, Y. Vitasse, G. Hoch, C. Körner. Growth and carbon relations of temperate deciduous tree
563 species at their upper elevation range limit. *J. Ecol.* 102, 1537–1548 (2014).

- 564 34. Q. Zeng, S. Rossi, B. Yang, C. Qin, G. Li, Environmental drivers for cambial reactivation of Qilian
565 junipers (*Juniperus przewalskii*) in a semi-arid region of northwestern China. *Atmosphere* 11, 232
566 (2020).
- 567 35. P. Ren, E. Ziaco, S. Rossi, F. Biondi, P. Prislan, E. Liang, Growth rate rather than growing season
568 length determines wood biomass in dry environments. *Agr. Forest Meteorol.* 271, 46–53 (2019).
- 569 36. P. Sanginés De Cárcer, Y. Vitasse, J. Peñuelas, V. E. J. Jassey, A. Buttler, C. Signarbieux, Vapor–
570 pressure deficit and extreme climatic variables limit tree growth. *Global Change Biol.* 24, 1108–1122
571 (2017).
- 572 37. J. Zhang, X. Gou, M. R. Alexander, J. Xia, F. Wang, F. Zhang, Z. Man, N. Pederson. Drought limits
573 wood production of *Juniperus przewalskii* even as growing seasons lengthens in a cold and arid
574 environment. *Catena* 196, 104936 (2021).
- 575 38. J. Huang, A. Deslauriers, S. Rossi, Xylem formation can be modeled statistically as a function of
576 primary growth and cambium activity. *New Phytol.* 203, 831–841 (2014).
- 577 39. S. Rossi, H. Morin, A. Deslauriers. Causes and correlations in cambium phenology: towards an
578 integrated framework of xylogenesis. *J. Exp. Bot.* 63, 2117–2126 (2012).
- 579 40. S. Rossi, M. J. Girard, H. Morin. Lengthening of the duration of xylogenesis engenders
580 disproportionate increases in xylem production. *Global Change Biol.* 20, 2261–2271 (2014).
- 581 41. H. E. Cuny, C. B. K. Rathgeber, D. Frank, P. Fonti, H. Mäkinen, P. Prislan, S. Rossi, E. M. Del
582 Castillo, F. Campelo, H. Vavrčík, J. J. Camarero, M. V. Bryukhanova, T. Jyske, J. Gričar, V. Gryc, M.
583 De Luis, J. Vieira, K. Čufar, A. V. Kirilyanov, W. Oberhuber, V. Trembl, J. Huang, X. Li, I. Swidrak,
584 A. Deslauriers, E. Liang, P. Nöjd, A. Gruber, C. Nabais, H. Morin, C. Krause, G. King, M. Fournier,
585 Woody biomass production lags stem-girth increase by over one month in coniferous forests. *Nat.*
586 *Plants.* 1, 15160 (2015).
- 587 42. E. Pasho, J. J. Camarero, S. M. Vicente-Serrano, Climatic impacts and drought control of radial
588 growth and seasonal wood formation in *Pinus halepensis*. *Trees.* 26, 1875–1886 (2012).

- 589 43. T. F. Keenan, J. Gray, M. A. Friedl, M. Toomey, G. Bohrer, D. Y. Hollinger, J. W. Munger, J. O
590 Keefe, H. P. Schmid, I. S. Wing, B. Yang, A. D. Richardson, Net carbon uptake has increased through
591 warming-induced changes in temperate forest phenology. *Nat. Clim. Change*. 4, 598–604 (2014).
- 592 44. L. Chen, H. Hänninen, S. Rossi, N. G. Smith, S. Pau, Z. Liu, G. Feng, J. Gao, J. Liu, Leaf senescence
593 exhibits stronger climatic responses during warm than during cold autumns. *Nat. Clim. Change*. 10,
594 777–780 (2020).
- 595 45. C. Körner. Paradigm shift in plant growth control. *Curr Opin Plant Biol*. 25, 107–114 (2015).
- 596 46. B. Muller, F. Pantin, M. Genard, O. Turc, S. Freixes, M. Piques, Y. Gibon. Water deficits uncouple
597 growth from photosynthesis, increase C content, and modify the relationships between C and growth
598 in sink organs. *J. Exp. Bot.* 62, 1715–1729 (2011).
- 599 47. N. D. Charney, F. Babst, B. Poulter, S. Record, V. M. Trouet, D. Frank, B. J. Enquist, M. E. K. Evans,
600 Observed forest sensitivity to climate implies large changes in 21st century North American forest
601 growth. *Ecol. Lett.* 19, 1119–1128 (2016).
- 602 48. Q. Liu, S. Piao, I. A. Janssens, Y. Fu, S. Peng, X. Lian, P. Ciais, R. B. Myneni, J. Peñuelas, T. Wang.
603 Extension of the growing season increases vegetation exposure to frost. *Nat. Commun.* 9, 426 (2018).
- 604 49. A. Deslauriers, H. Morin, Intra-annual tracheid production in balsam fir stems and the effect of
605 meteorological variables. *Trees*. 19, 402–408 (2005).
- 606 50. S. Piao, X. Wang, T. Park, C. Chen, X. Lian, Y. He, J. W. Bjerke, A. Chen, P. Ciais, H. Tømmervik,
607 R. R. Nemani, R. B. Myneni, Characteristics, drivers and feedbacks of global greening. *Nat. Rev.*
608 *Earth Environ.* 1, 14–27 (2020).
- 609 51. M. Huang, S. Piao, P. Ciais, J. Peñuelas, X. Wang, T. F. Keenan, S. Peng, J. A. Berry, K. Wang, J.
610 Mao, R. Alkama, A. Cescatti, M. Cuntz, H. De Deurwaerder, M. Gao, Y. He, Y. Liu, Y. Luo, R. B.
611 Myneni, S. Niu, X. Shi, W. Yuan, H. Verbeeck, T. Wang, J. Wu, I. A. Janssens, Air temperature
612 optima of vegetation productivity across global biomes. *Nat. Ecol. Evol.* 3, 772–779 (2019).
- 613 52. T. F. Keenan, W. J. Riley, Greening of the land surface in the world's cold regions consistent with
614 recent warming. *Nat. Clim. Change*. 8, 825–828 (2018).

- 615 53. J. J. Camarero, J. M. Olano, A. Parras, Plastic bimodal xylogenesis in conifers from continental
616 Mediterranean climates. *New Phytol.* 185, 471–480 (2010).
- 617 54. Y. H. Fu, S. Piao, H. Zhao, S. Jeong, X. Wang, Y. Vitasse, P. Ciais, I. A. Janssens, Unexpected role of
618 winter precipitation in determining heat requirement for spring vegetation green-up at northern middle
619 and high latitudes. *Global Change Biol.* 20, 3743–3755 (2014).
- 620 55. X. Wu, X. Li, H. Liu, P. Ciais, Y. Li, C. Xu, F. Babst, W. Guo, B. Hao, P. Wang, Y. Huang, S. Liu, Y.
621 Tian, B. He, C. Zhang, Uneven winter snow influence on tree growth across temperate China. *Global*
622 *Change Biol.* 25, 144–154 (2018).
- 623 56. X. Wang, T. Wang, H. Guo, D. Liu, Y. Zhao, T. Zhang, Q. Liu, S. Piao, Disentangling the
624 mechanisms behind winter snow impact on vegetation activity in northern ecosystems. *Global Change*
625 *Biol.* 24, 1651–1662 (2018).
- 626 57. H. D. Adams, A. D. Collins, S. P. Briggs, M. Vennetier, L. T. Dickman, S. A. Sevanto, N. Garcia-
627 Forner, H. H. Powers, N. G. McDowell, Experimental drought and heat can delay phenological
628 development and reduce foliar and shoot growth in semiarid trees. *Global Change Biol.* 21, 4210–
629 4220 (2015).
- 630 58. W. He, H. Liu, Y. Qi, F. Liu, X. Zhu, Patterns in nonstructural carbohydrate contents at the tree organ
631 level in response to drought duration. *Global Change Biol.* 26, 3627–3638 (2020).
- 632 59. A. P. Williams, C. D. Allen, A. K. Macalady, D. Griffin, C. A. Woodhouse, D. M. Meko, T. W.
633 Swetnam, S. A. Rauscher, R. Seager, H. D. Grissino-Mayer, J. S. Dean, E. R. Cook, C.
634 Gangodagamage, M. Cai, N. G. McDowell, Temperature as a potent driver of regional forest drought
635 stress and tree mortality. *Nat. Clim. Change.* 3, 292–297 (2012).
- 636 60. Y. Vitasse, A. Bottero, M. Cailleret, C. Bigler, P. Fonti, A. Gessler, M. Lévesque, B. Rohner, P.
637 Weber, A. Rigling, T. Wohlgemuth. Contrasting resistance and resilience to extreme drought and late
638 spring frost in five major European tree species. *Global Change Biol* 25, 3781–3792 (2019).
- 639 61. S. Zhao, N. Pederson, L. D'Orangeville, J. HilleRisLambers, E. Boose, C. Penone, B. Bauer, Y. Jiang,
640 R. D. Manzanedo, The International Tree-Ring Data Bank (ITRDB) revisited: Data availability and
641 global ecological representativity. *J. Biogeogr.* 46, 355–368 (2019).

- 642 62. F. Babst, B. Poulter, P. Bodesheim, M. D. Mahecha, D. C. Frank, Improved tree-ring archives will
643 support earth-system science. *Nat. Ecol. Evol.* 1, 8 (2017).
- 644 63. A. J. Elmore, S. M. Guinn, B. J. Minsley, A. D. Richardson, Landscape controls on the timing of
645 spring, autumn, and growing season length in mid-Atlantic forests. *Global Change Biol.* 18, 656–674
646 (2012).
- 647 64. S. A. Kannenberg, J. T. Maxwell, N. Pederson, L. D'Orangeville, D. L. Ficklin, R. P. Phillips Drought
648 legacies are dependent on water table depth, wood anatomy and drought timing across the eastern US.
649 *Ecol. Lett.* 22, 119–127 (2018).
- 650 65. S. Rossi, A. Deslauriers, T. Anfodillo, V. Carraro. Evidence of threshold temperatures for xylogenesis
651 in conifers at high altitudes. *Oecologia* 152, 1-12 (2007).
- 652 66. S. Gao, R. Liu, T. Zhou, W. Fang, C. Yi, R. Lu, X. Zhao, and H. Luo, Dynamic responses of tree-ring
653 growth to multiple dimensions of drought. *Global Change Biol.* 24, 5380–5390 (2018).
- 654 67. D. M. P. Peltier, K. Ogle, Tree growth sensitivity to climate is temporally variable. *Ecol. Lett.* 23,
655 1561–1572 (2020).
- 656 68. M. Wilmking, M. Maaten Theunissen, E. Maaten, T. Scharnweber, A. Buras, C. Biermann, M.
657 Gurskaya, M. Hallinger, J. Lange, R. Shetti, M. Smiljanic, M. Trouillier, Global assessment of
658 relationships between climate and tree growth. *Global Change Biol.* 26, 3212–3220 (2020).
- 659 69. K. Seftigen, D. C. Frank, J. Björklund, F. Babst, B. Poulter, The climatic drivers of normalized
660 difference vegetation index and tree-ring-based estimates of forest productivity are spatially coherent
661 but temporally decoupled in Northern Hemispheric forests. *Global Ecol. Biogeogr.* 27, 1352–1365
662 (2018).
- 663 70. A. G. Bunn, A dendrochronology program library in R (dplR). *Dendrochronologia.* 26, 115–124
664 (2008).
- 665 71. R Development Core Team. R: A language and environment for statistical computing. R Foundation
666 for statistical computing. (Vienna, Austria, 2019). <https://www.R-project.org/>
- 667 72. J. Sheffield, G. Goteti, E. F. Wood, Development of a 50-Year High-Resolution Global Dataset of
668 Meteorological Forcings for Land Surface Modeling. *J. Clim.* 19, 3088-3111 (2006).

- 669 73. P. L. Frich, P. Alexander, B. Della-Marta, M. Gleason, A. Haylock, K. Tank, T. Peterson, Observed
670 coherent changes in climatic extremes during the second half of the twentieth century, *Clim. Res.*, 19,
671 193–212 (2002).
- 672 74. G. T. Selyaninov, About climate agricultural estimation (in Russian). *Proc. Agric. Meteorol.*, 20, 165–
673 177 (1928).
- 674 75. D. L. Streiner, Finding Our Way: An Introduction to Path Analysis. *Can. J. Psychiatry*. 50, 115–122
675 (2005).
- 676 76. J. Fox, Z. Nie, J. Byrnes, sem: Structural Equation Models. R package version 3.1-9. 2017 Available
677 from: <https://CRAN.R-project.org/package=sem>
- 678 77. M. Iturbide, J. M. Gutiérrez, L. M. Alves, J. Bedia, R. Cerezo-Mota, E. Gimadevilla, A. S. Cofifño,
679 A. D. Luca, S. H. Faria, I. V. Gorodetskaya, M. Hauser, S. Herrera, K. Hennessy, H. T. Hewitt, R. G.
680 Jones, S. Krakovska, R. Manzanas, D. Martínez-Castro, G. T. Narisma, I. S. Nurhati, I. Pinto, S. I.
681 Seneviratne, B. van den Hurk, C. S. Vera. An update of IPCC climate reference regions for
682 subcontinental analysis of climate model data: definition and aggregated datasets. *Earth Syst. Sci.*
683 *Data* 12, 2959–2970 (2020).
- 684 78. R. P. Bagozzi, Y. Yi, Specification, evaluation, and interpretation of structural equation models. *J.*
685 *Acad. Market. Sci.* 40, 8–34 (2012).